

The Optical Gravitational Lensing Experiment. Catalog of high proper motion stars towards the Magellanic Clouds*

I. Soszyński¹, K. Żebruń¹, A. Udalski¹,
P. R. Woźniak², M. Szymański¹, M. Kubiak¹,
G. Pietrzyński^{3,1}, O. Szewczyk¹, and Ł. Wyrzykowski¹

¹Warsaw University Observatory, Al. Ujazdowskie 4, 00-478 Warszawa, Poland
e-mail:

(soszynsk,zebrun,udalski,msz,mk,pietrzyn,szewczyk,wyrzykow)@astrouw.edu.pl

² Los Alamos National Observatory, MS-D436, Los Alamos NM 85745, USA
e-mail: wozniak@lanl.gov

³ Universidad de Concepción, Departamento de Física, Casilla 160-C,
Concepción, Chile

ABSTRACT

We present a Catalog of high proper motion (HPM) stars detected in the foreground of central parts of the Magellanic Clouds. The Catalog contains 2161 objects in the 4.5 square degree area towards the LMC, and 892 HPM stars in the 2.4 square degree area towards the SMC. The Catalog is based on observations collected during four years of the OGLE-II microlensing survey. The Difference Image Analysis (DIA) of the images provided candidate HPM stars with proper motion as small as 4 mas/yr. These appeared as pseudo-variables, and were all measured astrometrically on all CCD images, providing typically about 400 data points per star. The reference frame was defined by the majority of background stars, most of them members of the Magellanic Clouds. The reflex motion due to solar velocity with respect to the local standards of rest is clearly seen. The largest proper motion in our sample is 363 mas/yr. Parallaxes were measured with errors smaller than 20% for several stars.

1 Introduction

Proper motions are of considerable value for finding faint nearby stars and studying overall galactic structure. Several groups undertook the proper motion surveys searching for white dwarfs and other low luminosity stars in the Galactic halo (e.g. Scholz *et al.* 2000, Wroblewski and Costa 2001, Nelson *et al.* 2001, Oppenheimer *et al.* 2001). The proper motions provided by the Hipparcos mission (Perryman *et al.* 1997) were already used to study local Galactic structure (Dehnen and Binney 1998).

The majority of hitherto existing HPM star catalogs are based on blinking pairs of photographic plates with several decades epoch difference. For example

*Based on observations obtained with the 1.3 m Warsaw telescope at the Las Campanas Observatory of the Carnegie Institution of Washington.

New Luyten Two-Tenths (NLTT) Catalog (Luyten 1979, Luyten and Hughes 1980), contains about 59 000 stars with proper motions larger than 0.18 arc-sec/yr. It is the result of comparing images taken at epochs separated by more than thirty years. NLTT and the majority of other catalogs of stars with proper motion contain objects found in uncrowded sky regions, as it is difficult to recognize the same HPM star in a crowded environment.

Eyer and Woźniak (2001) proposed a new method of finding HPM stars after a relatively short observation period (several years) in very crowded regions. The advantage of this method is that HPM stars are detected as a by-product of a search for variable stars, i.e. no additional effort is required. The method is based on the Difference Image Analysis (DIA) – image subtraction algorithm developed by Alard and Lupton (1998) and Alard (2000), and implemented by Woźniak (2000). Further details of the DIA analysis of the OGLE-II data may be found in papers by Woźniak (2000) and by Żebruń, Soszyński and Woźniak (2001). A star which changed its position relative to the reference frame defined by the majority of background stars usually appears as a pair of variables separated by one PSF (typically ~ 3 pixels). One component of the pair monotonically increases its brightness, while the brightness of the other component decreases correspondingly, with the total flux remaining constant.

Eyer and Woźniak (2001) proposed a simple model that provides a good estimate of the direction and the value of stellar proper motion, based on the measured rate of flux variation and the total flux of a candidate for a HPM star. The value of proper motion is given as

$$\mu = \frac{\sqrt{2\pi}\sigma}{F_{tot}}\gamma \quad (1)$$

where γ is the slope of the light curve, F_{tot} is the total flux, and σ is the dispersion of the PSF. The disadvantage of this method is a fact that F_{tot} often cannot be measured precisely. Therefore, it is important to perform astrometric measurements of the candidate HPM star, to have a more robust determination of its proper motion. In other words, the DIA software is very good in selecting HPM candidates, but it has to be supplemented with astrometry.

In this paper we present the results of a search for HPM stars, and the results of astrometry in the data obtained by the OGLE-II during four seasons of observations of the central parts of the Magellanic Clouds. We detected 2161 HPM stars towards the LMC and 892 stars towards the SMC. We present coordinates, proper motions and standard *BVI* photometry for all the HPM stars. All data presented in this paper are available from the OGLE Internet archive.

2 Observational Data

The observations were collected during the second phase of the OGLE experiment with the 1.3-m Warsaw telescope located at the Las Campanas Observatory, Chile (operated by the Carnegie Institution of Washington). The telescope was equipped with the "first generation" camera with a SITe 2048×2048 CCD detector working in the driftscan mode. The pixel size was $24 \mu\text{m}$ giving the $0.417 \text{ arcsec/pixel}$ scale. Observations of the LMC were performed in the "slow" reading mode of the CCD detector with the gain $3.8 \text{ e}^-/\text{ADU}$ and readout noise about 5.4 e^- . Details of the instrumentation setup can be found in Udalski, Kubiak and Szymański (1997).

Regular observations of the LMC fields started on January 6, 1997, while observations of the SMC started on June 26, 1997. About 4.5 square degrees of central parts of the LMC (21 fields) and about 2.4 square degrees of the SMC (11 fields) were observed during four seasons. Data collected up to the end of May 2000 were used to detect HPM stars.

From 260 to 510 *I*-band observations were collected for each of the LMC fields, and about 300 *I*-band observations for each of the SMC fields. For each of the LMC and SMC fields about 40 and 30 observations in the *V* and *B*-band, respectively, were also collected. The effective exposure time was 237, 173 and 125 seconds for *B*, *V* and *I*-band, respectively. Median seeing of the entire data set was about $1''.34$. The analysis was based on the *I*-band observations.

3 Selection of HPM stars

HPM stars appear in the difference images as a bipolar flux residuals changing approximately linearly over the entire period of observations. Light curves of the components of the residual pair are anti-correlated, because one of them is created in the area where light of star is reduced due to its motion, and the second is situated in this region where the light increases. Axis of the dipole fixes direction of the star velocity vector in the sky. The members of the pair are separated roughly by $1-1.5 \text{ arcsec}$, that is about 1 FWHM of the PSF. A simple model of the phenomenon was developed by Eyer and Woźniak (2001).

The DIA software can detect HPM star by registering both residual poles, or, depending on the adopted variability thresholds, only one member of the pair. In the second case a detection of a HPM star is more uncertain, as the DIA light curve may be due to genuine stellar variability. Furthermore, the identification of the DIA star on the reference frame may be difficult in some cases, as our fields are very crowded. In case of a pair of variables we searched for a star exactly in the middle of the pair. When only one component was detected we searched for a corresponding star on the reference frame within 1 arcsec of the DIA centroid.

Our selection of HPM stars among the DIA variable stars was divided into a few phases. First, we calculated a correlation function of light variations for each pair of close DIA variables, and we easily selected the pairs with anti-

correlated variability and separated by about $1 - 1.5$ arcsec. A significant majority of objects so selected turned out to be HPM stars.

To select HPM stars in the case of single monotonic variables we examined the shapes of their light curves. We were looking for objects with linear variability during four observational seasons by calculating correlations between light curves of already detected HPM stars and every remaining variable objects. Finally, we checked whether the corresponding star could be found in the reference image in distance of half FWHM (about $0.5 - 1$ arcsec).

Astrometric measurements were made for all candidates for HPM stars chosen in both ways. Again we used programs of DIA package. The large $2k \times 8k$ frames were subdivided into 512×128 pixel subframes, and next subframes which contain a given HPM star were re-sampled to the pixel grid of the OGLE template frame. When all of the subframes were in the same grid, we employed the DoPhot (Schechter, Mateo & Saha 1995) to measure pixel coordinates of the moving star. The last step was transforming X-Y coordinates to the equatorial coordinates. We used standard OGLE methods based in transformation derived with the Digitized Sky Survey image (for details see Udalski *et al.* 1998).

4 Model fit

Relative position of a star with respect to the background stars may change not only due to its proper motion. There are at least two phenomena which change the centroid position of stars with a one-year period. One of them is the parallactic motion, which depends on the distance to the star, the other is a differential refraction offset – second order effect of atmospheric refraction, caused by a difference in star color compared to the average color of reference stars. The effect changes the apparent zenith angle of the star and it is proportional to $\tan(z)$.

The differential refraction is correlated with the time of the year, because the zenith angle of observed regions is correlated with the time of the year. At the beginning of the observational season frames are taken right above the eastern horizon, in mid-season most of the observation are being conducted at minimal possible values of the zenith angle, and in the end of the season we observe again at large zenith angles right above western horizon. The refraction always moves the star toward the zenith, but according to the place in the sky, this is different direction in the equatorial coordinates. Dependence of differential refraction on the time of the year makes measuring a parallax of the star very difficult.

Nevertheless we tried to reckon differential refraction and parallaxes of the discovered HPM stars, because in several cases it was explicitly seen, that yearly oscillations were superposed on the monotonic motion in the sky (Fig. 1). To extract the parallax and the differential refraction effects we prepared a model of these phenomena, and fitted it to the measured coordinates of the stars.

To obtain the dependence between the differential refraction coefficient and the color of the star we measured positions of several thousand stars from the LMC and the SMC. These objects are distant enough to assume that proper

motions and parallaxes are undetectable. We used only bright ($I < 17$), rather isolated stars. For every observational point of the HPM star we computed the zenith angle and the parallactic angle, and determined expected differential refraction shift in RA and Dec directions. Next, using the least square method, we fitted the value to the measured positions of the object.

Fig 2 presents the diagram of color–differential refraction coefficient for every analyzed HPM star. As expected there is a clearly seen correlation between the color of the star and value of differential refraction shift. We determined linear relationship of these values and for HPM stars with known (V-I) color index and we corrected their coordinates for differential refraction.

The star’s coordinates in the sky at the time t can be described as follows:

$$\alpha = \mu_\alpha t + \pi \sin \gamma \sin \beta + r \tan z \sin p + \alpha_0 \quad (2)$$

$$\delta = \mu_\delta t + \pi \sin \gamma \cos \beta + r \tan z \cos p + \delta_0 \quad (3)$$

where α and δ are respectively right ascension and declination of the star, π is the parallax, r is the differential refraction coefficient, γ is an angular distance to the Sun in the celestial sphere, z is a zenith angle, β and p are angles in the celestial sphere between direction of respectively parallax shift and refractive shift and direction to the celestial North pole, finally α_0 and δ_0 are constant.

Knowing time t of every observation we computed values of γ , z , β and p . The position of the Sun was computed using formulae for the Sun position by van Flandern and Pulkkinen (1979). The differential refraction coefficient r was estimated using linear $r-(V-I)$ dependence. Next, using least square method we obtained values of μ_α , μ_δ , π , α_0 and δ_0 .

5 Results

Final list of HPM stars consists of 2161 objects found towards the LMC and 892 stars found in a foreground of the SMC. Using our method we could measure proper motions as small as 4 mas/yr. We note, that the method is insensitive to proper motions larger than ~ 1 arcsec/yr, because light curves of the components of the residual pair would quickly become constant.

Because the large number of objects in the catalog decided to make data available only in the electronic form. The lists of the HPM stars can be accessed *via* anonymous ftp at the following addresses:

<ftp://bulge.princeton.edu/ogle/ogle2/hpm/>
<ftp://sirius.astroww.edu.pl/ogle/ogle2/hpm/>

The ASCII files contain equatorial coordinates, measured proper motions, I -band photometry, $V-I$ and $B-V$ colors of all discovered HPM stars in the lines of sight to the LMC and the SMC. The tables contain more lines than the number of discovered HPM stars, because 55 objects towards the LMC, and 10 stars towards the SMC were detected twice – at the overlapping parts of adjacent fields.

The WWW interface of the catalog is available at the addresses:

<http://bulge.princeton.edu/~ogle/ogle2/hpm/>

<http://www.astroww.edu.pl/~ogle/ogle2/hpm/>

Apart from basic information about the stars, one can see here finding charts for every objects in the catalog and diagrams with the astrometric measurements of the stars.

In Figs. 3 and 4 we present location and motion vectors of all discovered HPM stars and contours of the observed fields. It can be seen that in a foreground of fields covering central part of the LMC (fields LMC_SC2–LMC_SC7) we discovered on average more HPM stars than towards the remaining LMC fields. This inhomogeneous density of detected HPM stars can be explained by different number and different period of observations. OGLE-II had collected about 500 *I*-band observations of fields LMC_SC2–LMC_SC7, and about 250–350 observations for fields covering regions outside strict center of the LMC. Regular observations of these fields started about six month after LMC_SC2–LMC_SC7. Shorter time baseline used for analysis probably caused that on the variability maps, created by DIA, some HPM stars remained below thresholds.

Color magnitude diagrams of the HPM stars from the catalog are presented in Fig. 5. Tiny dots indicates CMD diagrams of the background LMC and SMC stars. In Fig. 6 we present reduced proper motion diagram for our HPM stars. Reduced proper motion ($m + 5 \log \mu$) is a rough approximation of the absolute magnitude ($M = m + 5 \log \pi + 5$) up to a zero point offset.

Figs. 7 and 8 presents two-dimensional distribution of the proper motion vectors from the catalog. It is clearly seen, that stars prefer moving in the specified directions: roughly to the North in the foreground of the LMC and roughly to the East in the SMC regions. Average proper motion of the stars is more than 20 mas/yr, so it could not be an effect of proper motion of the Magellanic Clouds, because it is less than 2 mas/yr. Probably it is an effect of Solar movement relative to the local standard of rest. Simple calculations confirm this hypothesis. Assuming that the Sun is moving toward Hercules constellation ($\alpha = 18^h$, $\delta = +30^\circ$), nearby stars in the foreground of the LMC and SMC should move in the sky in the directions indicated with the arrows in Figs. 7 and 8.

In Table 1 we present parallaxes, positions, proper motions and magnitudes of stars, for which the parallaxes were measured with errors smaller than 20%. We found 25 such stars in the foreground of the LMC and 13 towards the SMC.

6 Completeness of the Catalog

One should note that we discovered the HPM stars using methods worked out for variable stars detection, not for searching fast moving objects. Therefore a completeness of the HPM catalog strictly depends on an efficiency of these algorithms. The DIA programs are finding variable objects with the PSF similar to the PSF of stars. Shapes of each member of the HPM residual dipole are only roughly similar to the PSF of stars, so we know for certain, that part

Table 1

Stars with measurable parallaxes. Errors of the parallaxes are smaller than 20%.

Field	Star ID	RA (J2000)	DEC (J2000)	π [mas]	μ_{α^*} [mas/yr]	μ_{δ} [mas/yr]	I [mag]	$V-I$ [mag]	$B-V$ [mag]
LMC_SC1	2000-2001	5 ^h 33 ^m 26 ^s .28	-69°48'26''8	9	41	65	15.923	2.844	1.664
LMC_SC2	273-274	5 ^h 31 ^m 02 ^s .19	-70°16'43''0	9	-7	-70	15.304	2.489	2.173
LMC_SC3	1246-0	5 ^h 28 ^m 41 ^s .98	-69°59'42''1	9	-36	-3	17.114	3.779	-
LMC_SC3	3350-0	5 ^h 28 ^m 30 ^s .58	-69°37'29''0	8	-5	-18	16.300	3.239	1.139
LMC_SC4	2134-0	5 ^h 26 ^m 45 ^s .90	-69°51'04''0	10	-28	-81	14.701	2.330	1.303
LMC_SC4	3877-0	5 ^h 25 ^m 45 ^s .02	-69°30'29''8	9	45	-93	15.318	2.455	1.453
LMC_SC4	4246-4247	5 ^h 27 ^m 07 ^s .14	-69°26'37''6	9	-1	-22	16.101	2.855	1.574
LMC_SC4	4539-4541	5 ^h 27 ^m 31 ^s .33	-69°22'09''6	16	79	134	14.718	3.718	1.383
LMC_SC6	3491-3492	5 ^h 20 ^m 43 ^s .13	-69°22'46''6	12	32	118	16.607	3.484	-
LMC_SC6	4307-0	5 ^h 22 ^m 33 ^s .42	-69°12'02''6	8	-32	16	13.892	2.383	1.645
LMC_SC7	429-0	5 ^h 18 ^m 58 ^s .28	-69°47'47''5	9	67	113	13.342	2.484	1.341
LMC_SC8	532-533	5 ^h 17 ^m 26 ^s .10	-69°41'21''2	17	106	155	14.794	3.569	1.152
LMC_SC8	1411-1413	5 ^h 16 ^m 44 ^s .98	-69°29'30''3	19	-131	217	13.574	3.515	1.563
LMC_SC9	1361-1362	5 ^h 12 ^m 49 ^s .43	-69°18'37''6	7	78	8	13.926	2.415	1.579
LMC_SC9	2148-0	5 ^h 13 ^m 23 ^s .89	-69°06'02''2	25	-34	46	16.366	4.478	-
LMC_SC9	2497-2498	5 ^h 12 ^m 40 ^s .08	-68°58'30''3	22	-45	75	15.489	3.595	1.333
LMC_SC12	1245-1246	5 ^h 05 ^m 56 ^s .07	-69°22'59''9	9	13	-30	13.438	2.476	1.433
LMC_SC12	1367-1368	5 ^h 05 ^m 44 ^s .54	-69°19'21''7	11	27	-7	14.205	2.606	1.432
LMC_SC13	351-352	5 ^h 05 ^m 26 ^s .99	-69°04'54''8	20	108	99	14.233	3.409	-
LMC_SC13	2914-2915	5 ^h 07 ^m 04 ^s .47	-68°18'31''4	10	-35	-82	14.165	2.797	1.413
LMC_SC16	700-701	5 ^h 35 ^m 19 ^s .34	-70°15'23''8	14	-9	-74	14.432	2.756	1.538
LMC_SC16	1263-1264	5 ^h 35 ^m 41 ^s .03	-70°03'31''5	10	-7	31	13.979	2.478	1.554
LMC_SC21	592-593	5 ^h 20 ^m 07 ^s .30	-70°35'31''8	25	-44	242	15.204	3.384	1.864
LMC_SC21	667-0	5 ^h 20 ^m 16 ^s .60	-70°32'40''6	16	-14	40	15.213	3.170	1.857
LMC_SC21	1241-0	5 ^h 21 ^m 05 ^s .67	-70°12'42''0	16	55	34	13.980	2.346	1.822
SMC_SC3	210-211	0 ^h 42 ^m 50 ^s .17	-73°29'19''6	11	48	-93	13.784	2.189	1.625
SMC_SC4	1681-0	0 ^h 46 ^m 12 ^s .77	-72°50'25''1	12	-51	-23	13.729	2.585	-
SMC_SC5	370-0	0 ^h 49 ^m 00 ^s .99	-73°26'06''9	12	75	44	15.408	2.822	1.732
SMC_SC7	61-62	0 ^h 55 ^m 59 ^s .74	-73°19'19''0	15	-142	-57	14.985	2.735	1.865
SMC_SC7	759-0	0 ^h 55 ^m 38 ^s .47	-72°58'01''5	12	40	13	14.692	2.459	1.523
SMC_SC7	1403-0	0 ^h 54 ^m 51 ^s .69	-72°38'24''4	15	47	-46	14.175	2.647	1.638
SMC_SC7	1539-1540	0 ^h 55 ^m 56 ^s .30	-72°34'34''8	13	37	-24	13.812	2.780	1.549
SMC_SC8	934-935	1 ^h 00 ^m 10 ^s .42	-72°30'14''2	8	-158	-155	15.021	2.467	1.798
SMC_SC10	375-376	1 ^h 04 ^m 49 ^s .97	-72°28'57''8	22	352	-90	15.461	3.195	1.833
SMC_SC10	631-632	1 ^h 03 ^m 56 ^s .50	-72°05'57''1	17	59	-16	14.987	2.923	1.725
SMC_SC11	156-0	1 ^h 06 ^m 39 ^s .91	-72°55'07''2	9	-27	-25	16.362	2.973	-
SMC_SC11	551-552	1 ^h 09 ^m 09 ^s .19	-72°35'43''4	8	86	12	15.616	2.765	1.533
SMC_SC11	780-0	1 ^h 08 ^m 10 ^s .29	-72°25'03''4	15	86	8	16.895	3.809	-

$$\mu_{\alpha^*} = \mu_{\alpha} \cos \delta$$

of the HPM stars in our fields were not detected. The fact that only less than half of HPM candidates had both poles of a pseudo variable pair detected with the DIA implies that there were some HPM stars for which neither pole was detected, and the object was missed.

In Fig. 9 we present I -band magnitudes plots against the proper motions. It is clearly visible, that there is a minimal value of proper motion, below which star's movement cannot be detected using our methods. We registered proper motions as small as 4 mas/yr for stars of $I = 14 \div 16$ mag. For brighter and especially fainter stars the detection limit is higher.

Fig. 3 shows that the completeness of the catalog strongly depends on a number and time-span of observations. Density of the HPM stars, which should be independent of background LMC stars, is significantly higher in more frequently observed regions. Therefore we consider that the completeness of the HPM sample is higher in the fields LMC_SC2–LMC_SC7 than in other fields.

Recently Alcock *et al.* (2001) detected 154 HPM stars along the lines of sight of the Galactic Bulge and the Large Magellanic Cloud, selecting them from the MACHO catalog of variable stars. The catalog contains stars with proper motion larger than 30 mas/yr. Towards the LMC, 64 HPM stars were detected, 20 of which are in the line of sight of OGLE fields. In the SMC MACHO collaboration detected one HPM star. We conducted cross identification of the stars in both catalogs, during which we found out that 19 HPM stars were rediscovered (18 stars in the LMC and 1 star in the SMC). One of not detected stars was too bright ($I = 12.4$) and stayed just above our saturation level. The other star has been missed, because correlation coefficient between shapes of the residual poles and the PSF of the stars was too low.

We obtained about 80% completeness of the stars with $\mu > 30$ mas/yr and $I < 17$ mag by comparing the HPM stars in the overlapping regions in the neighboring fields. One should note that regions at the field edges are biased by smaller number of observations, due to imperfections in telescope pointing, what reduces the completeness of the catalog in these areas. In total 33 stars with $\mu > 30$ mas/yr should be paired with counterparts in the overlapping fields. We found counterparts in 27 cases. When we compared subsample of stars with proper motion larger than 50 mas/yr, we identified all counterparts in the neighboring fields. The completeness of the catalog is decreasing for fainter stars and with smaller proper motion. We estimate that for objects with proper motion smaller than 10 mas/yr, the completeness is less than 50%.

7 Conclusions

Difference Image Analysis offers a great possibility of detecting HPM stars in dense stellar regions. The moving stars are discovered in the procedure of variable star detection, so the process does not require any special efforts.

The knowledge of stars in the Solar neighborhood is the starting point for projects of determining stellar luminosity and mass functions and other properties of stars. Large number of HPM stars in this catalog will be useful to study

Galactic dynamics. Many of the objects are undoubtedly low-luminosity stars, such as M-dwarfs. These stars are hot topics, because their features are still a matter of debate.

HPM stars in a foreground of densely crowded stellar fields offer possibility for predicting lensing events many years in advance. Paczyński (1996) showed that astrometric effect of gravitational microlensing, which can be measured by Hubble Space Telescope, may enable a direct mass determination for the neighboring stars. The cross-section for astrometric effect is larger than the cross-section for photometric effect of gravitational microlensing measurable from the ground. It means that predictions of microlensing by stars from the HPM catalogs may significantly increase the number of targets for astrometric measurements from space.

The Space Interferometry Mission (SIM) telescope, planned to be launched in 2009, will allow to measure positions in the sky with about $4 \mu\text{as}$ accuracy. It could permit the determination of the distance, mass and radius of the lensing object (Paczynski 1998). Gould (2000) and Salim & Gould (2000) discussed the selection of candidates for SIM observations.

Third phase of OGLE project (OGLE-III) started in June, 2001. The telescope has been equipped with a new generation CCD mosaic camera 8192×8192 pixels, what considerably increased quality of the images. We expect that OGLE-III data will allow to detect proper motions as small as 1-2 mas/yr, and to determine exact parallaxes of the neighboring stars.

Acknowledgments. We would like to thank Prof. Bohdan Paczyński for many discussions and support in this work. This work was partly supported by the KBN grant 5P03D02520 to I. Soszyński and 2P03D01418 to M. Kubiak. Partial support was also provided by the NSF grant AST-9830314 to B. Paczyński. Support for PW was provided by the Laboratory Directed Research and Development funds at LANL.

REFERENCES

- Alard, C., and Lupton, R. H. 1998, *Astrophys. J.*, **503**, 325.
- Alard, C. 2000, *Astron. Astrophys. Suppl. Ser.*, **144**, 363.
- Alcock, C. *et al.* 2001, *Astrophys. J.*, **562**, 337.
- Dehnen, W., and Binney, J. J. 1998, *MNRAS*, **298**, 387.
- Eyer, L., and Woźniak, P. R. 2001, *MNRAS*, **327**, 601.
- Gould, A. 2000, *Astrophys. J.*, **532**, 936.
- Luyten, W. J. 1979, *New Luyten Catalogue of Stars with Proper Motions Larger than Two Tenths of an Arcsecond* (Minneapolis: Univ. Minnesota Press).
- Luyten, W. J., and Hughes, H. S. 1980, *Proper Motion Survey with the Forty Eight Inch Schmidt Telescope, First Supplement to the NLTT* (Minneapolis: Univ. Minnesota Press).
- Nelson C. A., Cook K. H., Axelrod T. S., Mould J. R., and Alcock C. 2001, astro-ph/0112414.
- Oppenheimer, B. R., Hambly, N. C., Digby, A. P., Hodgkin, S. T., and Saumon, D. 2001, *Science*, **292**, 698.
- Paczyński, B. 1996, *Acta Astron.*, **46**, 291.
- Paczyński, B. 1998, *Astrophys. J.*, **494**, L23.
- Perryman, M. A. C. *et al.* 1997, *Astron. Astrophys.*, **323**, L49.
- Samir, S., and Gould, A. 2000, *Astrophys. J.*, **539**, 241.
- Schechter, P. L., Mateo, M. L., and Saha, A. 1995, *P.A.S.P.*, **105**, 1342.
- Scholz, R. D., Irwin, M., Ibata, R., Jahreiss, H., and Malkov, O. Yu. 2000, *Astron. Astrophys.*, **353**, 958.
- Udalski, A., Kubiak, M., and Szymański, M. 1997, *Acta Astron.*, **47**, 319.
- Udalski, A., Szymański, M., Kubiak, M., Pietrzyński, G., Woźniak, P. R., and Żebruń, K. 1998, *Acta Astron.*, **48**, 147.
- van Flandern, and T. C., Pulkkinen, K. F. 1979, *Astrophys. J. Suppl. Ser.*, **41**, 391.
- Woźniak, P. R. 2000, *Acta Astron.*, **50**, 421.
- Wroblewski H., and Costa E. 2001, *Astron. Astrophys.*, **367**, 725.
- Żebruń, K., Soszyński, I., and Woźniak, P. R. 2001, *Acta Astron.*, **51**, 303.

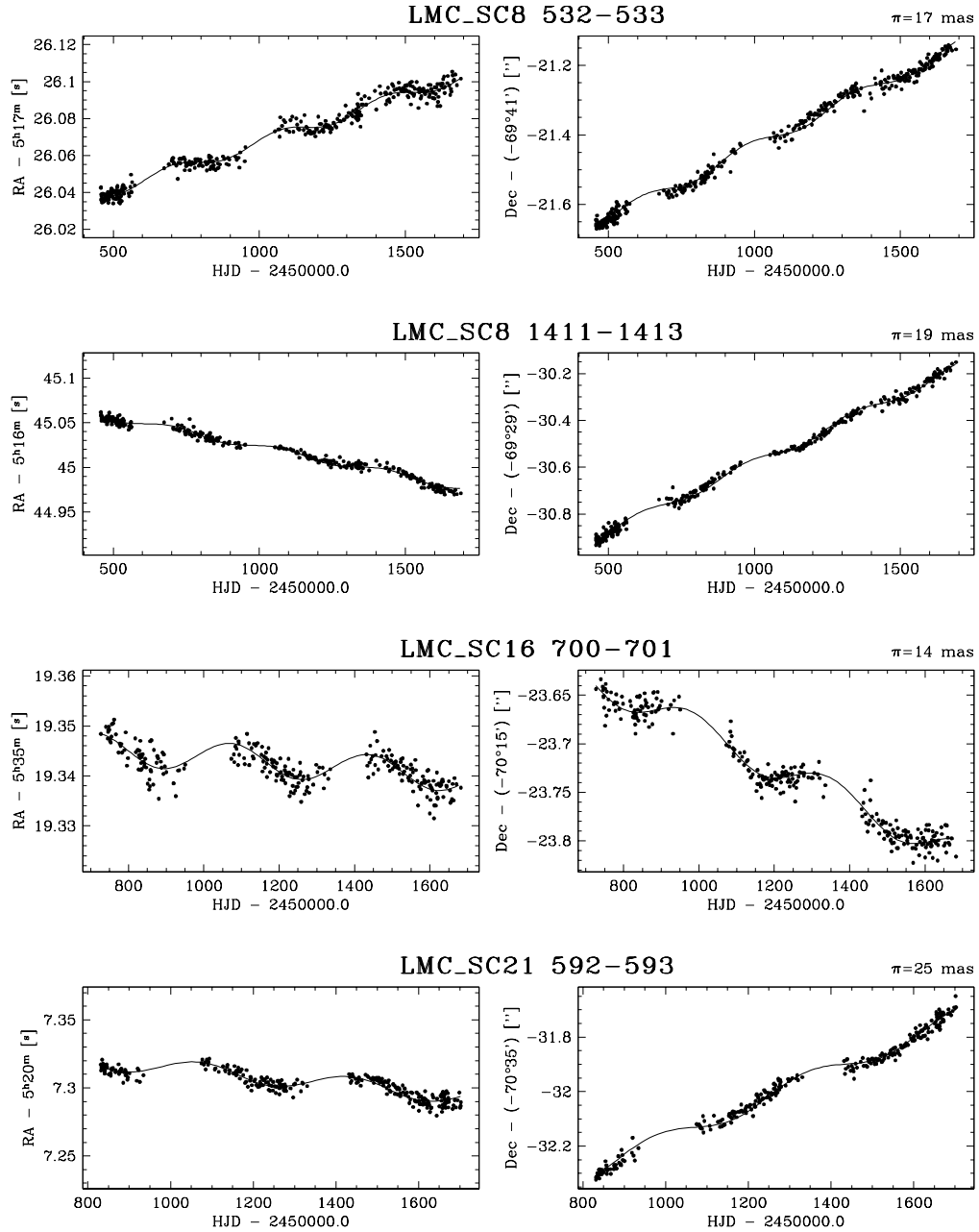


Fig. 1. Equatorial coordinates of the four HPM stars from the LMC with the model fit. The differential refraction shift is subtracted from every point.

Fig. 2. Correlation between the colors of stars and the fitted differential refraction coefficient for stars from the LMC (upper panel) and from the SMC (lower panel). The dispersion of these diagrams is an effect of local differences in background stars' color and uncertainties of the astrometric measurements.

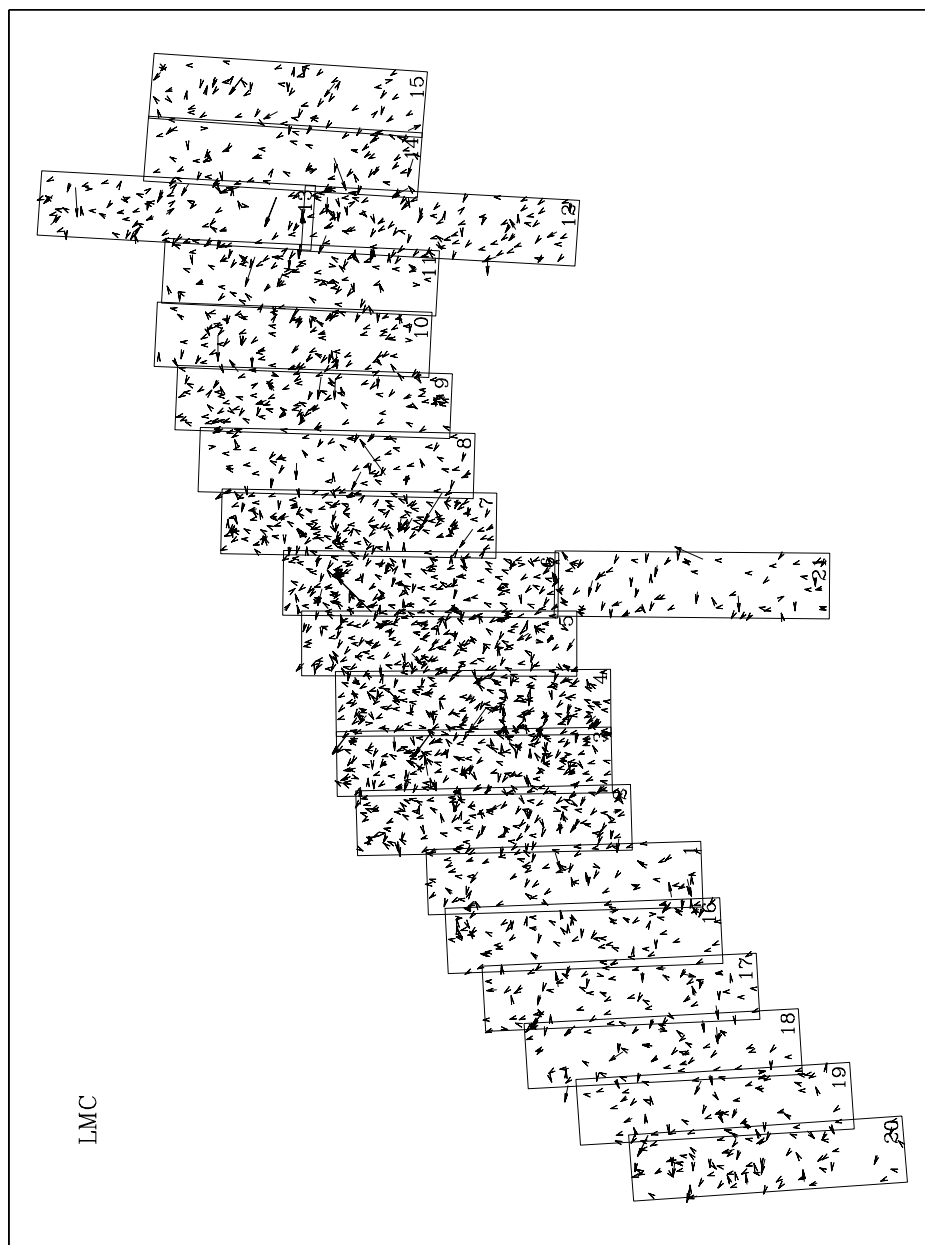


Fig. 3. Map of the LMC fields with discovered HPM stars.

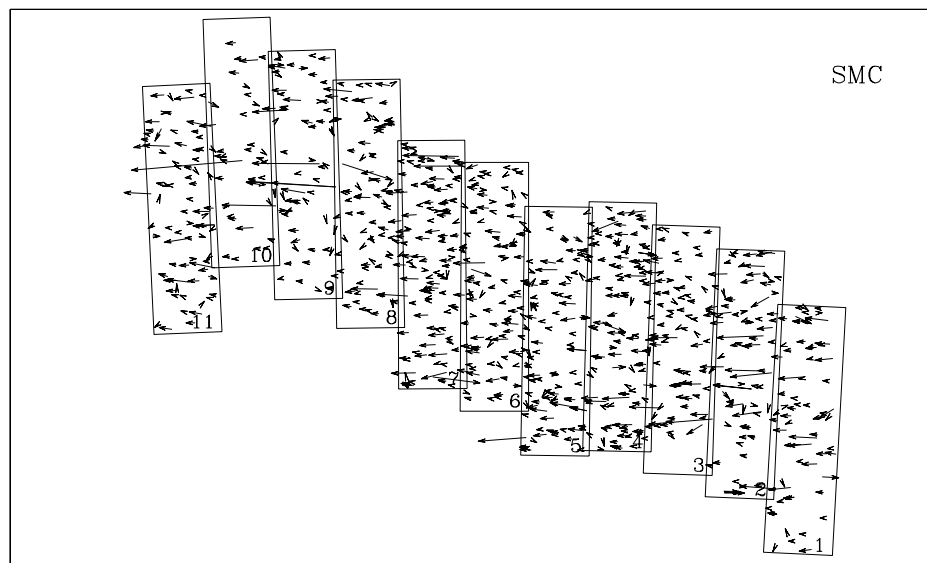


Fig. 4. Map of the SMC fields with discovered HPM stars.

Fig. 5. Color-Magnitude diagram of the HPM stars observed towards the LMC (upper panel) and the SMC (lower panel). Tiny dots in the upper and lower panel indicate about 50 000 stars from LMC_SC3 and SMC_SC1 fields respectively

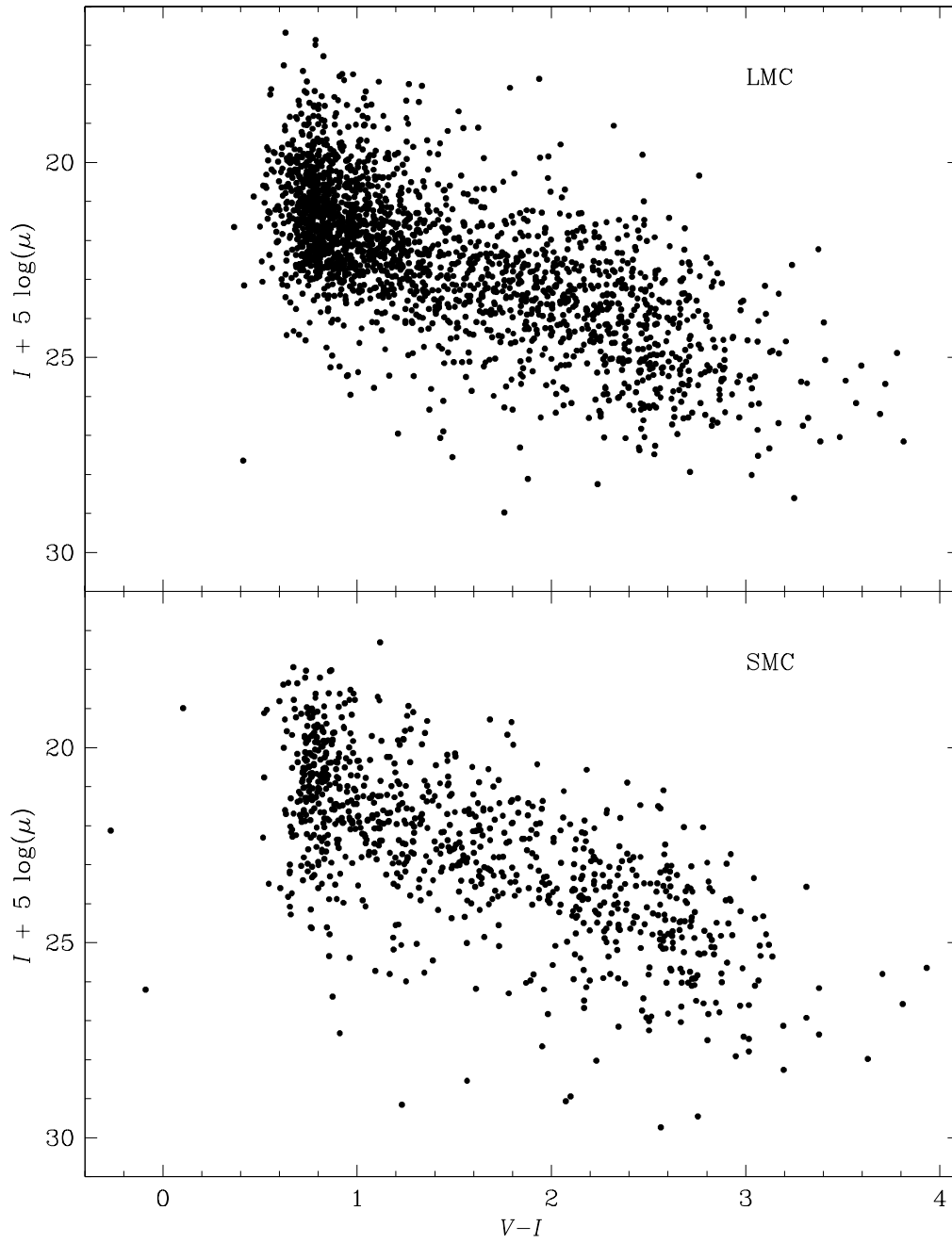


Fig. 6. Reduced proper motion diagram for HPM stars observed towards the LMC (upper panel) and the SMC (lower panel).

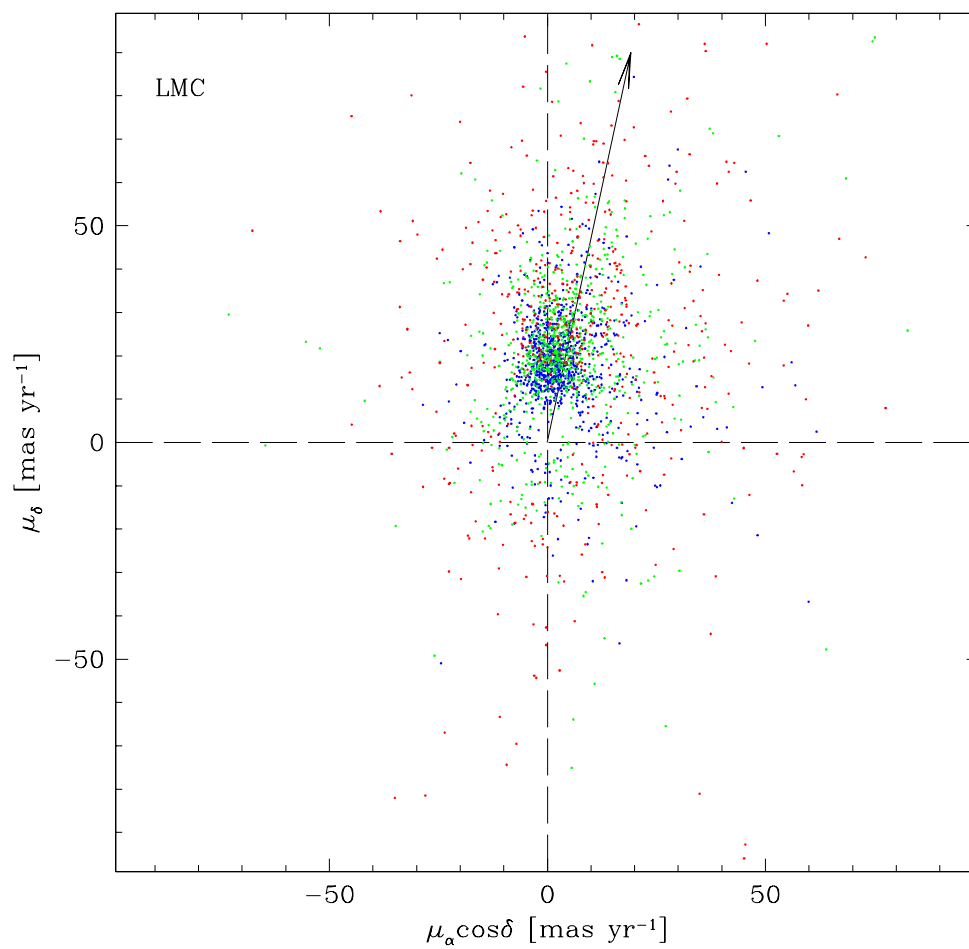


Fig. 7. Two-dimensional distribution of proper motions μ_α , μ_δ of stars towards the LMC. The long arrow shows the direction opposite to the solar apex. Colors of the points indicate colors of the stars – blue: $(V-I) < 1$, green: $1 < (V-I) < 2$ and red: $(V-I) > 2$.

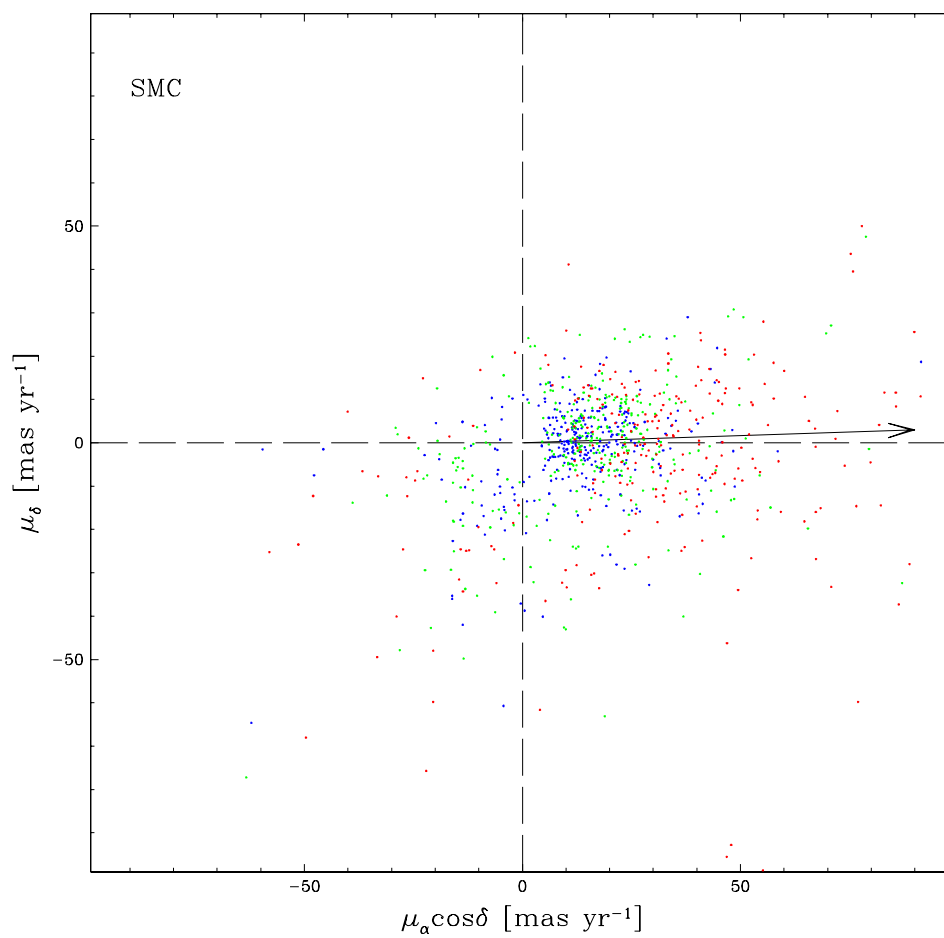


Fig. 8. Two-dimensional distribution of proper motions μ_α , μ_δ of stars towards the SMC. The long arrow shows the direction opposite to the solar apex. Colors of the points were described in the caption to Fig. 7

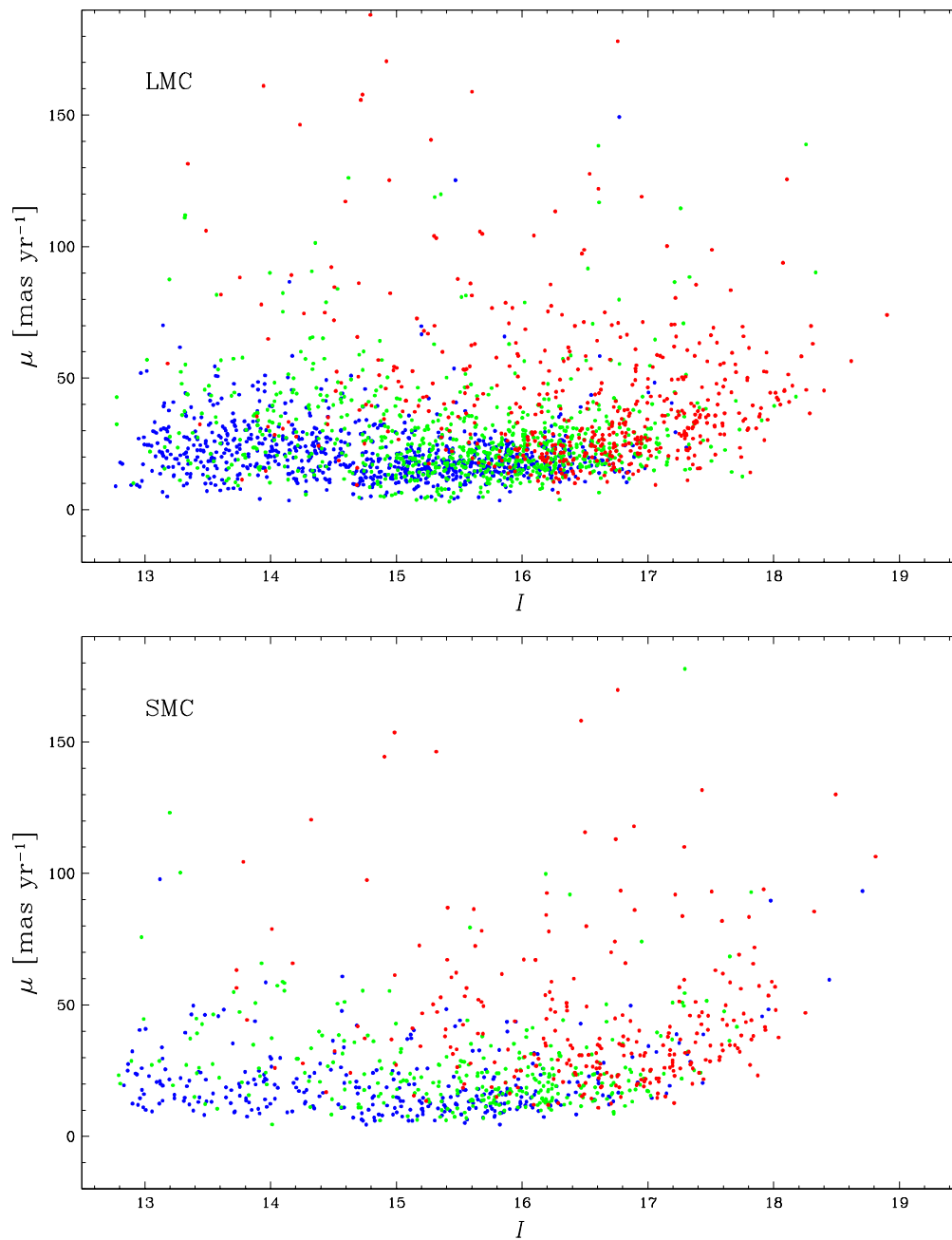


Fig. 9. Luminosity versus proper motion diagram of the HPM stars observed towards the LMC (upper panel) and the SMC (lower panel). One can notice dependence between minimal measured value of proper motions and magnitude of stars. Colors of the points were described in the caption to Fig. 7

This figure "fig2.jpg" is available in "jpg" format from:

<http://arxiv.org/ps/astro-ph/0205289v1>

This figure "fig5.jpg" is available in "jpg" format from:

<http://arxiv.org/ps/astro-ph/0205289v1>